Available online at www.worldscientificnews.com

World Scientific News

WSN 54 (2016) 267-288 EISSN 2392-2192

The Third Option for Stopping Cancer: Complex, Temporally Patterned Weak Magnetic Fields- Critical Factors That Influence Their Efficacy and Potential Mechanisms

Nirosha J. Murugan, Nicolas Rouleau, Michael A. Persinger*

Biomolecular Sciences Program, Laurentian University, Sudbury, Ontario, P3E 2C6, Canada

E-mail addresss: nx_murugan@laurentian.ca ; ny_rouleau@laurentian.ca ;
* mpersinger@laurentian.ca

ABSTRACT

One of the most promising technologies for suppressing the growth of malignant (cancer) cells without adversely affecting normal cells involves the application of physiologically-patterned and bioquantum compatible magnetic fields with specific temporal increments generated by optocoupler circuits through each of the three spatial planes. However, experimentally generated magnetic field patterns designed to target cancer cells are also immersed within the magnetic environment of the incubators. We measured anomalous alterations in the horizontal (primarily "east-west") component of the geomagnetic static field intensity within cell incubators when the most effective experimental field was being generated between three sets of solenoids. The eccentric response was a function of the six solenoids being wrapped or not wrapped with copper foil. In addition, activating or deactivating the experimental field for fixed increments was associated with discrete and obvious DC shifts in the horizontal component as well as emergent patterns that were not a component of either the experimental field or the background incubator 60 Hz source. If the temporal pattern that defines the effects induced by these magnetic fields is analogous to the spatial patterns that define chemical functions, failure to accommodate these anisotropic transients could be a source of the frequent contradictions and inter-laboratory failures to replicate these phenomena. We suggest that the emergent phenomena from these interactions with quantum-like features may be the causal variables responsible for many of the promising effects for cancer suppression. A modified Dicke model derived from quantum optics where cells cooperatively interact with a single mode of the field and their dipole fields interact coherently may accommodate the observed effects.

***Keywords*:** new treatments for malignancy; geomagnetic vector differences; interactions with patterned magnetic fields; cancer inhibition; copper blocking; Aharanov-Bohm applications; Dicke quantum optics application

1. INTRODUCTION

The central concept that manifested in late 19th and early 20th century chemistry was that molecular structure determined function. The complexity of the functions and the efficacy of any combinations of compounds upon biological systems were further complicated by the precise nature of the microenvironment in which the reaction occurred. The interface between molecules and the external surface of the living cell was realized to be a multivariable configuration. The specific consequences of introducing multiple chemical components within this microenvironment were a function of the molecular structure of the proteins that constituted the receptors, the competition between the many chemical species that were proximal to the reactions, and some measure of compatible resonance that influenced the likelihood of the dose-dependent interaction between the external field of the chemical structures and those expressed upon the cell membrane's surface.

Within the domain of magnetobiology and magnetochemistry, the appreciation for the precision required to produce powerful biological and chemical effects has been minimal. The term "magnetic field effects" is applied homogeneously as if all magnetic field applications are similar. This is analogous to applying a large number of structurally different molecular compounds that would produce different and even contradictory effects but still considering them the same or simply, "chemical effects". These inconsistencies reflect the precision of the geometries required to produce reliable results. Several theorists and experimenters (Adair, 1991; Berg, 1999; Murugan et al., 2015; Rouleau et al., 2016) have shown that the orientation of the static magnetic field, the local geomagnetic field configuration and the temporal, spatial, and intensity characteristics of the applied electromagnetic fields can affect and even determine the magnitude of effects. Our working hypothesis is that all components and origins of magnetic fields within the region where the exposures and measurements of biological systems occur must be measured and identified in order to discern which synergism is actually producing the significant effects.

Multiple examples of interactions between magnetic fields applied within the same space and time were elegantly described by Burke (1986). Intrinsic features include the Larmor frequency of a proton (proton resonance) which is within the range of cerebral and cell functions (40 Hz) when the applied field is within the μT range and of the electron which is within a similar frequency band (30 Hz) when the applied field is within the nT range. With multiple superimposition of magnetic fields a myriad of phenomena can emerge synergistically such as photomagnetic effects, inductive reactance (the characteristic of a coil to oppose current depending upon its rate of change and inductance), eddy currents, thermoelectric effects, intrinsic thermal gradients, and magnetoacoustic phenomena. Although the traditional proclivity is to simplify the exposure system this reduction in complexity also indicates fewer degrees of freedom for which specific interactions are required. Simplifying the geometry of magnetic field exposures for biomagnetic interactions might be considered analogous to attempting to ascertain the specificity of large molecular compounds by ignoring their complex configurations and using a "simple" substance such as water. The subsequent

modelling may be palatable and conceptually parsimonious but the effects would be both trivial and limited.

The importance of understanding synergisms between experimental and natural magnetic fields is not trivial. The contemporary treatment of most cancers and malignant cell growth is confined to either intense radiation or toxic chemotherapies. These procedures, although effective, frequently eliminate normal cells as well as malignant cells. In addition they result in significant cognitive compromise and untoward side effects that reduce the quality of life. We (Buckner, 2012; Karbowski et al., 2012) have found that applications of physiologically patterned, weak magnetic fields to dozens of different human and animal malignant cell lines reduce their proliferation by approximately 50% without influencing normal cells. In addition, the temporal patterns of these magnetic fields provide beneficial analgesic effects (Martin et al, 2004) without activating the molecular pathways through which morphine operates and metastases occurs (Afsharimani et al., 2011). Other researchers have found that complex-patterned magnetic fields with spectral power densities within the 8 to 25 Hz range retard or eliminate the growth of malignant cells *in vitro*. This optimal range had been discovered decades ago by Adey (1981) while studying calcium efflux across membranes. If physiologically-patterned magnetic fields are a third option to treat one of the most challenging conditions in the history of medicine and science, then understanding all of the nuances that can diminish their efficacy must be explored.

For example the presence of copper as shielding or shelving within cell culture incubator systems is remarkably common. However, sheets of this metal produce anomalous effects for which the total physical mechanism is not clear. Murugan et al (2015) exposed spring water (to simulate cell physiological conditions) to frequency-modulated, weak (1 microTesla) magnetic fields generated between two coils. One coil was activated and the other was not activated. The intention was to produce the potential conditions for a Bohm-Aharanov effect as well as a magnetic vector A. These researchers then measured the photon emissions from aliquots of that water once removed from the field. The glass containers that had been wrapped with aluminum, plastic or no material all showed markedly enhanced fluorescence photon emissions between 275 and 305 nm. The flux was a factor of 25 greater than photon emissions below or above this band. The containers of water wrapped with copper during the magnetic field exposure displayed complete abolishment of this emission band.

Karbowski et al (2016a) expanded the investigation of this phenomenon by exposing mouse melanoma (skin cancer) cells in plates between three pairs of solenoids (one pair in each spatial plane). They reiterated the descriptions of Tonomura et al (1986) who had nicely articulated the Aharanov-Bohm effects involving electron beams and copper shielding. Karbowski et al (2016a) predicted that a phase shift might occur between the opposite solenoids in a plane independent of the magnetic flux. They assumed an essential energy unit of 10^{-20} J (2010), the involvement of the Compton wavelength, and the time within the voltage field to be a unit electron orbit. The phase modulation required for this increment of energy with these parameters was about $1.5 \cdot 10^{-12}$ m per phase. When voltage was reconfigured, the optimal value to produce the Aharanov-Bohm effect was about 4.3 V.

This discrete voltage was within the range of the ± 5 V systems (Koren et al, 2015) employed to produce the effective suppression rates in the growth of cancer cells. Multiple experiments demonstrated that the titrated voltages applied through the circuitry to the solenoids to produce the greater inhibitory effects on malignant cell growth was 4.3 V. Values

below or above this precise number produced less or no suppression of malignant cell growth. When each solenoid was wrapped with copper foil the inhibitory effect upon malignant cells growth was completely abolished without affecting the intensity of the frequency-modulated, physiologically patterned magnetic field (Karbowski et al, 2016b). This reliable measurement suggested that the efficacy of time-varying magnetic fields reported by several authors (e.g., Karbowski et al, 2015) may involve variables sequestered within the domain of field intensity.

Zhadin et al (1998) succinctly demonstrated that DC magnetic fields applied orthogonally to time-varying fields produced differential effects. That stronger static fields and superimposed weaker, temporal fields should interact is not surprising. One of the most general phenomena in perceptual detection is Weber's Law which indicates that for a just noticeable difference to occur for a change in stimulus intensity there must be a specific (optimal) ratio between the intensity of the changing stimulus with respect to the background static (larger) stimulus. Many researchers assume that the resultant static magnetic field of the earth, upon and within which experimental magnetic fields are superimposed, is sufficient to describe immersive phenomena. However the total field is composed of three vector directions that can vary substantially while the resultant field remains more or less consistent. Each vector (plane) can display differential effects. As recently shown experimentally by Vares et al (2016) the human brain behaves as a dipole whose shifts in microVoltage as measured by quantitative electroencephalography are precisely the difference in torque (energy) between either aligned or orthogonal orientation with the N-S component of the field only.

These eccentric changes in the intensities of the field parameters when time-varying fields are immersed within the 60 Hz fields of copper-jacked incubators may be more important than assumed. Buckner et al (2015), Karbowski et al (2015) and several other groups of researchers have shown conclusively that appropriately patterned magnetic fields diminish the growth of several lines of malignant cells without affecting the growth of normal cells. This differential effect is qualitatively different from the effects of chemotherapy or radiation treatments that often kill both cancer and normal cells. Patterned magnetic field treatments penetrate the tissue and are not dependent upon vasculature for distribution within the tissue as is the case for chemotherapies. Here we present evidence: 1) of the importance of directionality and spatial plane in the production of the effective component of the applied field, 2) the differential effects of copper shielding of the solenoids that generate experimental magnetic fields, 3) how these fields inside of standard copper-shielded incubators results in marked alterations in the resulting intensity for exposures, and 4) that the Dicke model for quantum optics may serve as quantitative metaphor for central components of the magnetic field effects on malignant cell cultures.

2. METHODS AND MATERIALS

Our basic paradigm consisted of exposing a magnetometer sensor to a complex patterned electromagnetic field within a small exposure box typically used in experiments involving cancer cells. The box, equipped with solenoids, was placed within or outside of an incubator. The external surfaces of the solenoids were either partially covered or uncovered by copper wrapping which was designed to modify potential components within the

electromagnetic field exposure (see Figure 1) . The magnetometer sensor was exposed to combinations of these experimental conditions in addition to different temporal increments of exposure and inter-exposure periods. We hypothesized that combinations of these variables would affect the intensity as well as other components of the field exposures in ways which might enhance or decrease the experimental effects associated with our various biological paradigms.

Magnetometer Measurements

A MEDA FVM-400 Vector Magnetometer sensor was placed into a cubed enclosure (4D box) with solenoids affixed to the center of each surface (Figure 2). The 4D box device is typically used to expose malignant cell lines to patterned (Karbowski et al, 2015; Murugan et al, 2014a) electromagnetic fields – a protocol which has demonstrated considerable anti-cancer effects (Hu et al., 2010). A Lenovo laptop computer with a Windows 7 operating system was programmed to, using custom software, convert data strings into patterned current output which operated the 4D box solenoids (Koren et al, 2015). The standard decelerating frequency modulated, Thomas (a decelerating frquency modulated) electromagnetic field pattern (see Figure 3) which has been used in many experimental contexts in our laboratory was measured directly by the magnetometer and power meter.

The circuitry by which this pattern (and related patterns) are generated is a patented (Koren et al, 2015), custom constructed system (US Patent 7553272). In summary, the Thomas pattern is composed of 849 numbers each of which has a value between 0 and 256. They are converted by Digital to Analogue Convertors (DAC) to values between -5 and +5 V (127=0 V). The circuit is based upon a series of optocouplers and Triac components that allow photon transmissions across junctions to transform the input between -5 to +5 V. The potentials are delivered to approproriate pairs of solenoids such that all three planes of space are occupied. The point duration which is the time each number between 0 and 256 are activated to produce the specific voltage has been found to be critical for the effect. When each of the points are ~3 ms the resulting magnetic field significantly reduces malignant cell growth and optimally affects calcium flux densities within cells (Buckner et al, 2015). Point durations less or greather than this value are not effective. The duration of one presentation of the pattern composed of 839 numbers at 3 ms each is 2.52 s. This is repeated for the duration of the experimental exposure.

Field intensity (nT) values were obtained in increments of 1 second (1 Hz) across three axes: X, Y, and Z. The X-axis consisted of the horizontal plane parallel with the bottom of the incubator, running from the front to the back of the incubator. The Y-axis consisted of the same horizontal plane though the direction of the plane was perpendicular, running from one side (lateral wall) of the incubator to the other. The Z-axis was positioned within a plane perpendicular to both of the aforementioned planes, running from the bottom of the incubator to the top. The orientation of the magnetometer sensor was calibrated with respect to the X-axis at declination 20 deg. Consequently the orientation was slightly oblique. The exposure protocol was an A-B-A-B design where the field pattern was intiated and terminated multiple times within a trial. The time of each exposure (A) and the inter-exposure times (B) were always of equivalent temporal length. We selected four temporal increments of exposure: 5 sec, 10 sec, 20 sec, and 30 sec. This meant that, for example the Thomas field was activated for 10 s and deactivbated for 10 s for 5 pairs of repetitions. Trials were repeated in triplicate in order to determine both internal variability and reliability.

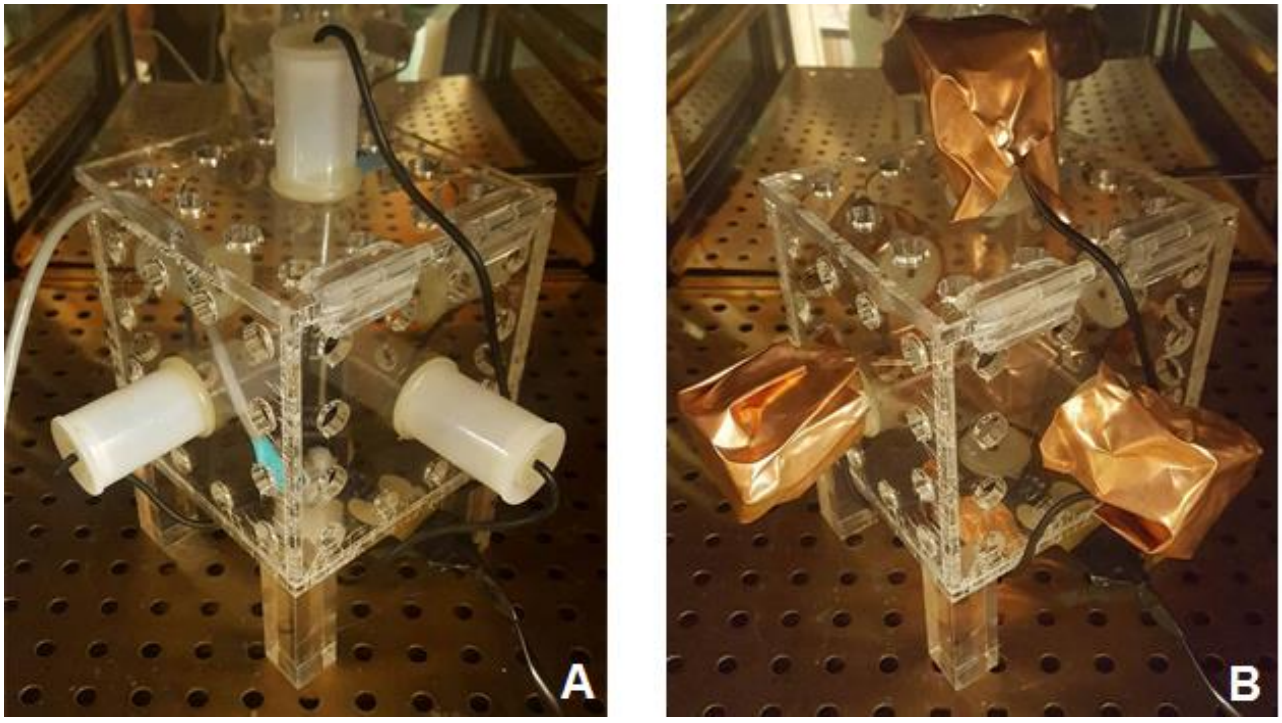

Figure 1. The 4D box within the incubator without (**A**) and with (**B**) copper-shielding surrounding the external surfaces of the solenoids.

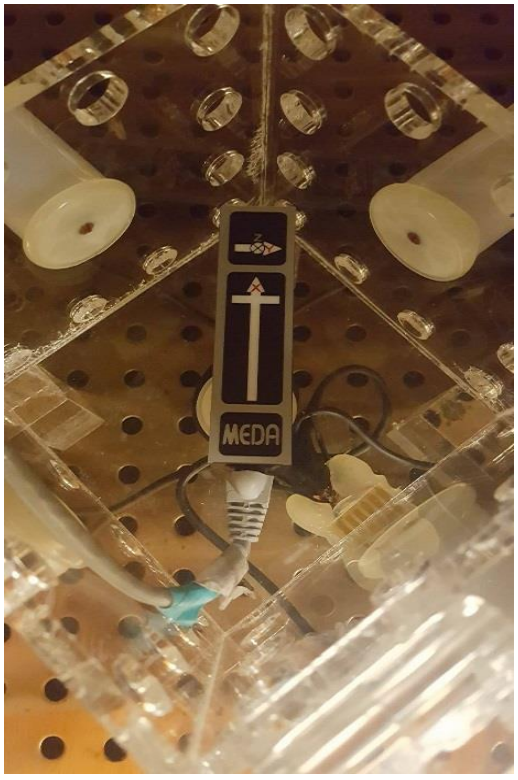

Figure 2. The FVM-400 sensor positioned within the 4D box within the incubator.

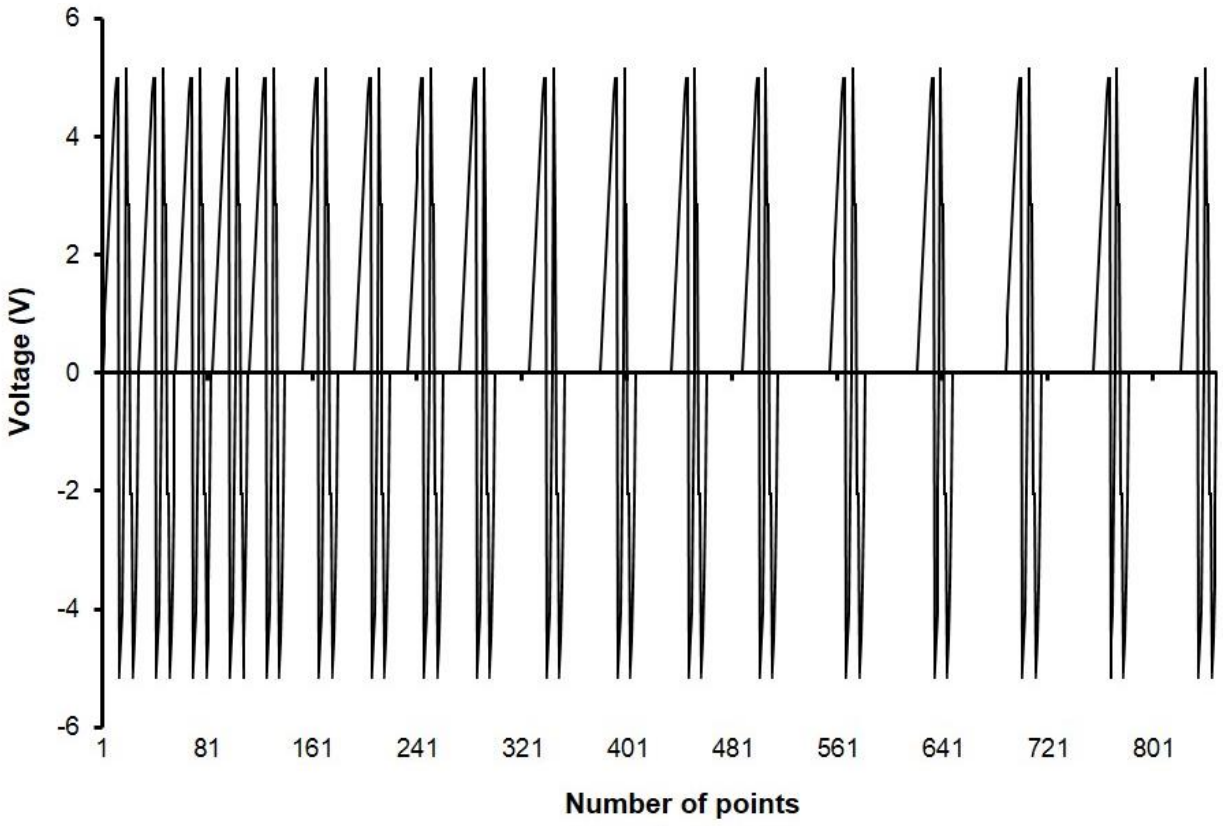

Figure 3. Pattern of the decelerating frequency modulated (Thomas) pattern that elicits more than 50% suppression of malignant cell growth in vitro. Vertical axis indicates voltage that was optimally ±4.3 V. Horizontal axis reflects time in 3 ms increments for a total of 859 points for a total of 2.58 s per cycle.

3. RESULTS

The measurements within and outside of the incubator when the copper wrapping of the solenoids were off or on are shown in Table 1. The data indicated that when the 4D box was placed within the incubator, the copper wrapping surrounding the solenoids attenuated the intensity of the background electromagnetic field (nT) by ~ 50% within the Y-axis relative to when the solenoids were uncovered. This effect was not noted when the 4D box was placed outside the incubator ($p>.05$). Effects associated with the other axes were subtle, and required further detailed analysis.

Measurements of Y-axis (Figure 4) field intensity as a function of alternative exposure and inter-exposure temporal increments revealed consistency across most conditions where copper-shielded boxes were generally associated with decreased field intensity relative to non-shielded boxes when placed inside the incubator ($p<.05$). Copper-shielding did not influence field intensity if the 4D box was placed outside of the incubator ($p>.05$). An anomalous effect was noted for the repeated 20 second exposure condition wherein copper shielding did not demonstrate the same field intensity diminishments when the 4D box was placed within the incubator.

Table 1. Average intensity measures for x-, y-, and z- axes as a function of 4D cell box exposure copper shielded vs non-shielded, and within or outside of the incubator. Note the 50% reduction in static field intensity for the y axis when shielded with copper.

Condition	Intensity (nT)					
	X-AXIS		Y-AXIS		Z-AXIS	
	Outside	Inside	Outside	Inside	Outside	Inside
Copper OFF	10007.6	102459.9	10609.18	25301.82	39773.86	50887.76
Copper ON	10078.94	104980.9	10945.42	12518.41	39633.64	46723.92
	% Difference					
	1.007129	1.024605	1.031694	0.494763	0.996475	0.918176

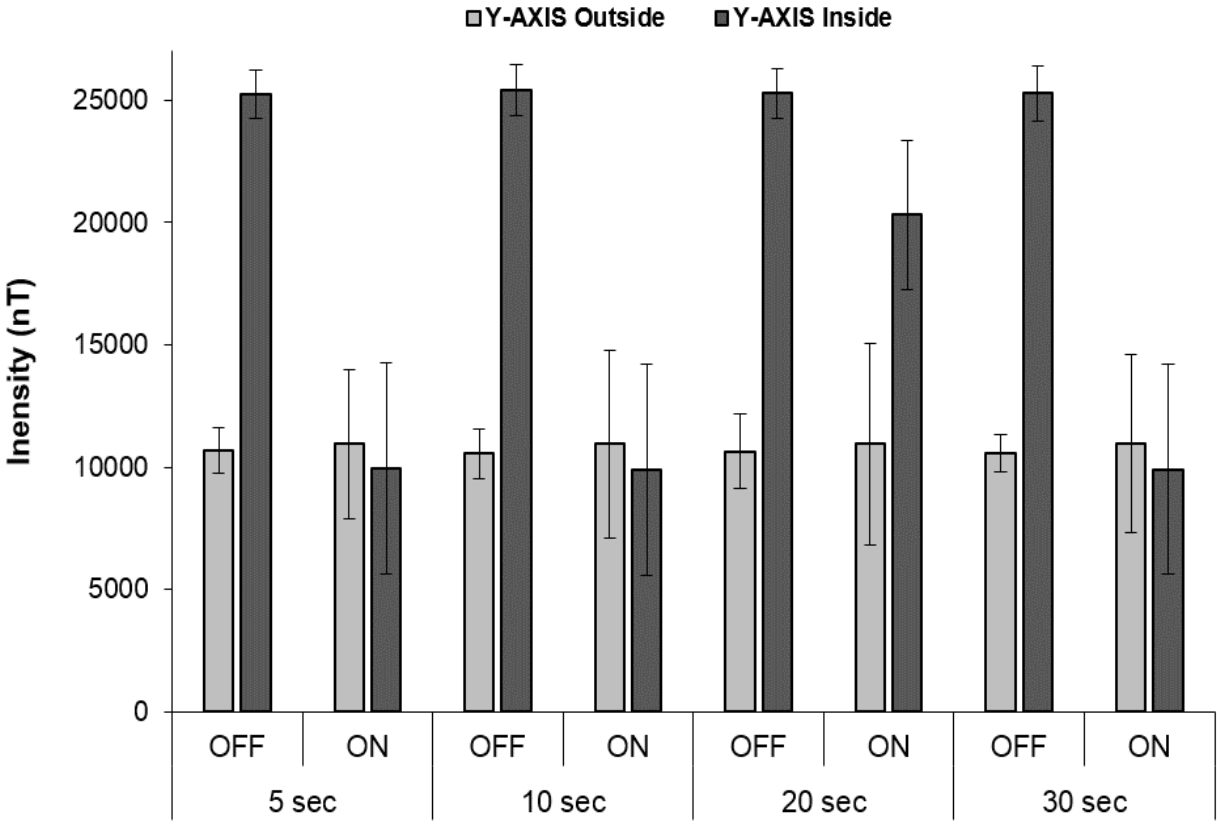

Figure 4. Comparison of the static magnetic field in 4D box shielded with (ON) and without (OFF) copper. It is apparent that application of copper shielding had the strongest effect inside of the incubator, where it reduced the background static magnetic field as compared to no shielding, in all time increments (except 20 seconds) where the copper weakened the effect.

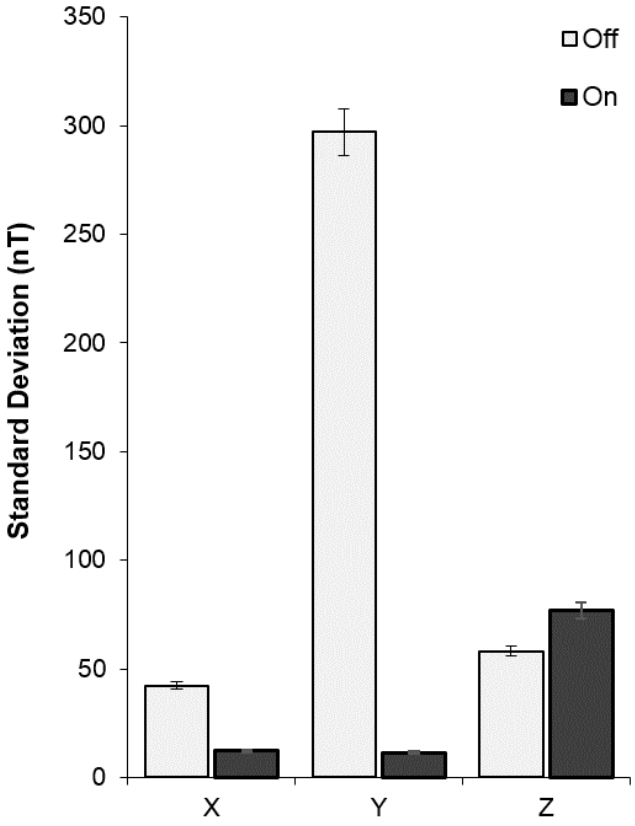

Figure 5. Standard deviation (variability) of field intensity (nT) as a function of X, Y, and Z planes as a function of whether the copper wrapping were either covering (On) or not covering (Off) the 4D box solenoids.

Variability was computed for strings of nT values measured during the presentation of the field (Figure 5). The solenoids were either covered (On) or uncovered (Off) by a copper wrapping. Clear increases in nT variability were noted for the uncovered solenoids relative to the copper-covered solenoids across the Y-axis of the probe [$t(78) = 26.65$, $p<.001$, $r^2 = .90$]. A similar increase in nT variability was noted for the uncovered solenoids relative to the copper-covered solenoids across the X-axis of the probe [$t(78) = 18.19$, $p<.001$, $r^2 = .81$]. However, an opposite effect was noted for the Z-axis where the uncovered solenoids were associated with significantly less nT variability relative to the copper-covered solenoids [$t(78) = -4.32$, $p<.001$, $r^2 = .19$]. "Variability" within a "steady-state" component of the geomagnetic field contribution has been considered to be a latent source of signals and related potential information that can affect biochemical reactions (Rouleau and Persinger, 2015). Figure 6 reflects the unexpected shifts in the steady-state component of the Y axis of the geomagnetic field (primarily east-west) when the experimental magnetic field was switched on or off for fixed durations. The smaller amplitude dense lines reflect the effects of the Thomas pulse (Figure 3). The configuration is not discernable because of the time scale. When the field was deactivated, there was compensatory steady-state overshoots that remained present (and

would affect cells immersed within it) until the experimental field was activated again. There was no systematic pattern with respect to the polarity of the steady-state shift.

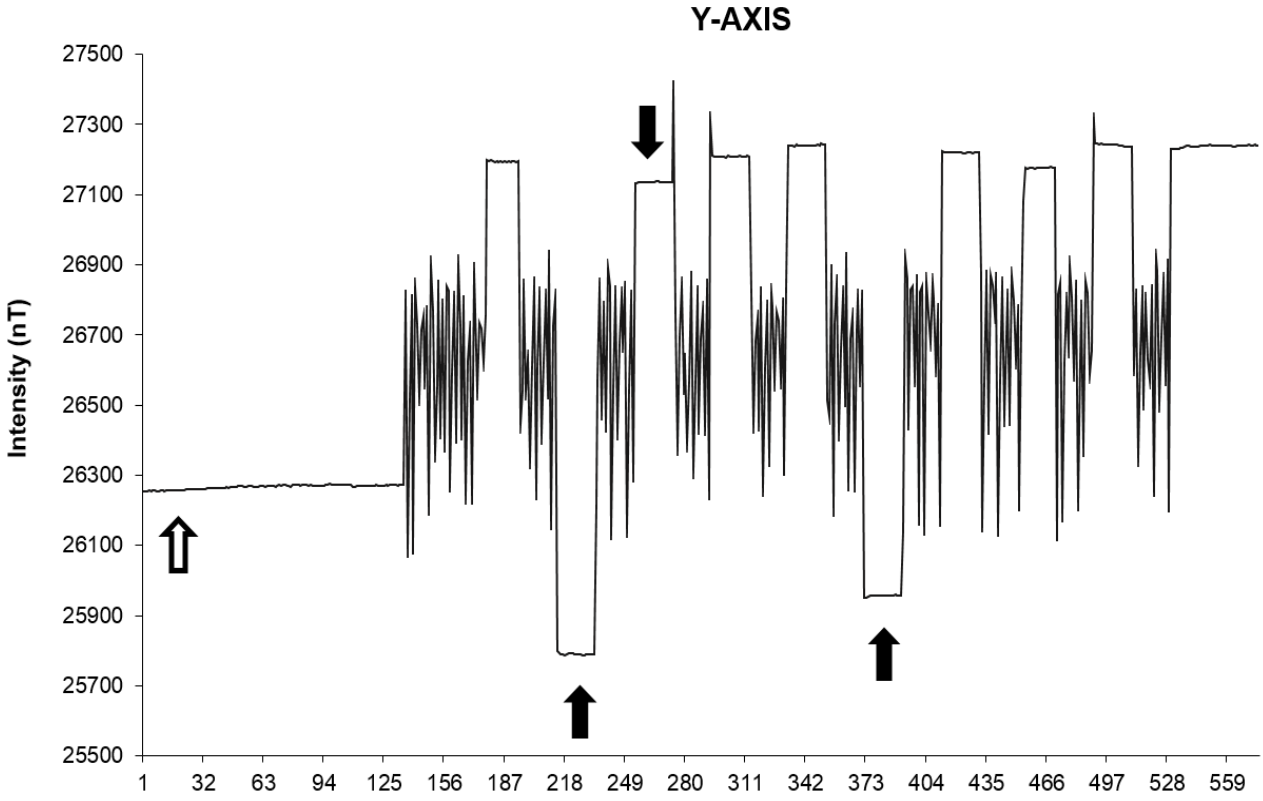

Figure 6. An example of field intensity directional reversals upon initiation and termination of the field exposure over time. The white arrow indicates baseline background field intensity measurements. The initiation of the first field exposure is indicated by the sharp increase in field intensity at ~ 130 seconds and subsequent high-frequency fluctuations at equal intervals through the trial. The square-shaped deviations as indicated by the black arrows are inter-exposure periods wherein the solenoids were turned off. Note that the baseline or background field intensity reverses direction with respect to the relatively static intensity associated with the electromagnetic field exposure.

Figure 7 illustrates the number of directional reversals of the steady state (geomagnetic) field when the experimental field was activated or deactivated for different durations outside of the incubator. The durations were 5 s, 10 s, 20 s and 30 s. The numbers of pairs of activation-deactivation were between 10 and 15. There was marked consistency within a specific duration. Two effects were notable. First, the number of deviations varied across the different durations of activation and deactivation. Secondly, for one interval (20 s) the presence of copper shielding around the solenoids produced the opposite effect than the other three intervals. When the exposure chamber was placed inside the incubator (Figure 8) this anomaly was eliminated for the 20 s on-off field presentation when the copper shielding around the solenoids was present or not.

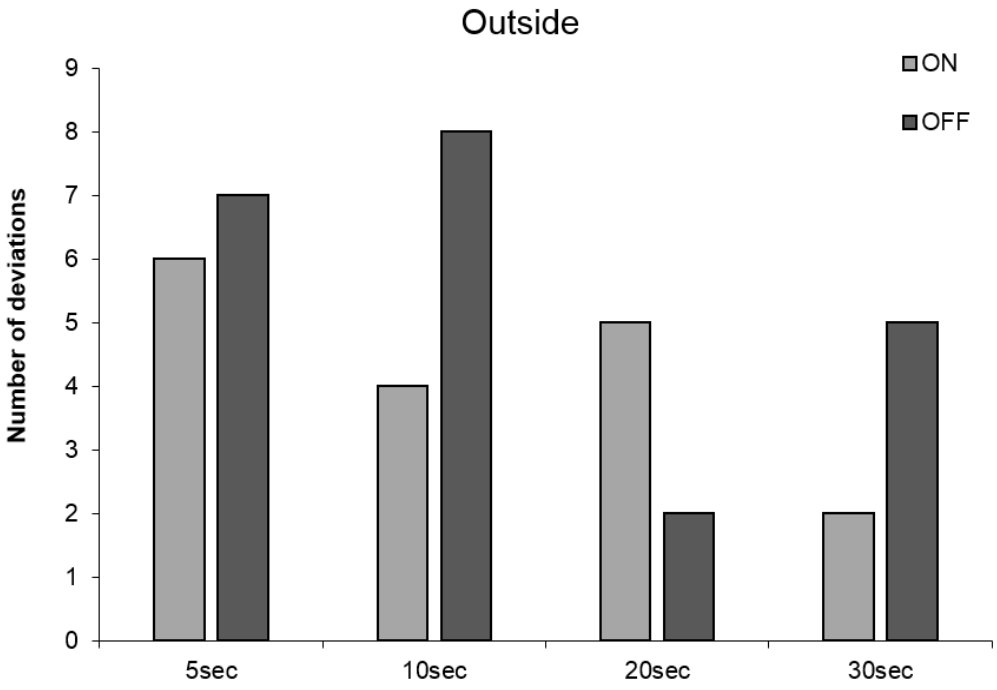

Figure 7. Number of directional reversals associated with field intensity changes (copper on or off) upon serial initiation and termination of the electromagnetic field as a function of the temporal increment of each exposure and inter-exposure period for trials completed within the 4D box positioned outside of the incubator.

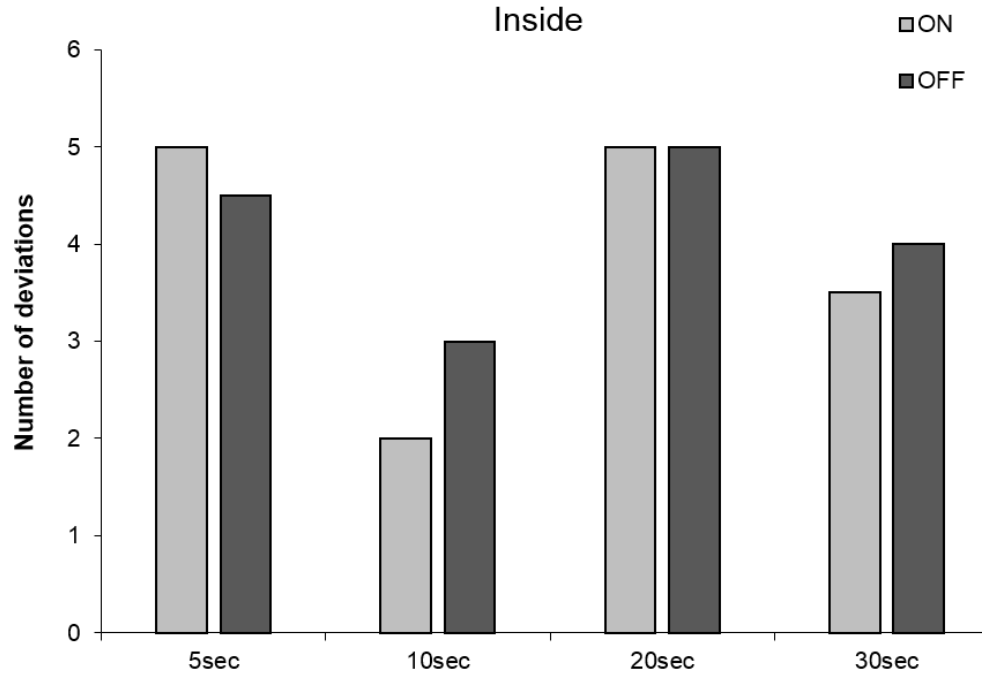

Figure 8. Number of directional reversals associated with field intensity changes (copper on or off) upon serial initiation and termination of the electromagnetic field as a function of the temporal increment of each exposure and inter-exposure period for trials completed within the 4D box positioned within the incubator.

4. DISCUSSION AND CONCLUSIONS

Researchers who study biochemistry or pharmacology are acutely aware of the importance of molecular structure. The specific spatial configuration of the molecule primarily determines its function although dynamics from the local environment contributes. The potential errors from assuming that all chemical structures behave the same because they share a phenol or indole ring despite different side chains or compositions would be obvious. However, some researchers over-include magnetic field effects as homogenous phenomena such that electromagnetic fields created by different sources, with different intensities, various spatial application geometries, and different temporal shapes are all considered "magnetic fields" with the implicit assumption of convergent similarity. The results of the experiments reported here indicate that large and unusual shifts in magnetic field intensities within specific planes can occur when magnetic fields are immersed within magnetic fields. Such anomalies may help explain the challenges of replication of the effects of "magnetic fields" upon cellular dynamics in general and the specific inhibition of malignant cells in particular.

There were three major observations that are relevant to exploring the efficacy of applying physiologically-patterned magnetic fields to suppress malignant cell growth such as melanoma. First, wrapping the solenoids (between which the fields were generated) with copper foil did not affect the static magnetic field strength compared to when the solenoids are not wrapped outside of incubators within the normal laboratory environment. This would be expected. There was also no appreciable difference in the values for the Z (vertical) component when the copper metal was wrapped around the solenoid or not and the exposure device was either outside or inside the incubator. When the exposure box was placed within the incubator there was an increase in the intensity of the Y component by a factor of 2. Inside the incubator the presence of the copper around the solenoids markedly reduced this enhancement.

From our perspective the most revealing measurement was the attenuation of the standard deviation or variability of the magnetic field strength during the conditions that are associated with the maximum reduction of malignant cell growth in our experiments. Standard deviation can be employed as an inference of variability of the "signal" within the field. As shown in Figure 6, activating and deactivating the Thomas pattern was associated with marked steady state shifts in the ambient geomagnetic field that was a greater intensity then the band of variation associated with the experimental magnetic field. We understand that these anomalous transients are generated by the circuitry of the Koren (Koren et al, 2015) digital-to-analogue system. However from the perspective of developing a reliable electromagnetic-field based technology to inhibit malignant cell growth, there are three potentially important observations and derivations.

First, the steady-state shift to produce either an enhanced or diminished geomagnetic ambient accompanied the termination of the experimental field and remained for the duration before the next pattern sequence was initiated. This could be considered the equivalents of "space-markers" containing information that facilitated the effect upon exposed cells. About 20 years ago, Litovitz et al (1997) completed a series of elegant experiments that have been unfortunately not appreciated for their profound significance. They found cells and central biochemical reactions associated with cellular processes such as ornithine decarboxylase activity demonstrated "temporal sensing". There were critical intervals for disrupting the constantly presented extremely low frequency electromagnetic fields that completely

abolished the responsiveness to these fields. If the interruptions were more than 100 ms the field-induced enhancement of ornithine decarboxylase activity was eliminated.

Second, the increased standard deviations in the steady-state transients that occurred when the "effective" experimental fields were off occurred in the horizontal plane (the X and Y components). This could explain an interesting discrepancy between the required spatial rotations associated with the malignant cell slowing effects required for mice compared to cell cultures. Hu et al (2010) and Buckner (2012) showed that daily exposures of mice injected with melanoma cells required the spatial rotation of the experimental field across each of the three planes separately and then the simultaneous presentation in all three planes. In this context the switch from X to Y to Z to XYZ planes occurred every 0.5 s such that one duty cycle was completed every 2 s. However, for cell culture exposures, the condition employed in the present experiment, all three planes remained activated; the spatial rotation was not required. The discrepancy for maximum effectiveness between mouse and cell may simply reflect the three dimensional (bulk volume) of the mouse compared to the two dimensional (effectively a thin sheet) of cells in culture.

If the latter assumption is valid, then perhaps the mechanism for the malignant cell growth suppression occurs because the effective variability in signals is applied through the thin sheet of cells rather than across the large cross-sectional area. The diameter of the standard cell culture dish is ~6 cm and contains 2.5 cc of malignant cells in suspension. This means that as they proliferate over the typical experimental duration of 5 to 6 days before they approach 100% confluence, the activity occurs within a thin sheet with a thickness of ~1 mm. Unlike an effect from cross section application where individual cells would be influenced by the field independently, generation of the critical component through the thin horizontal plane would allow each cell to contribute the influence from the field to each adjacent cell such that the conditions for the Dicke model (Garraway, 2011) could be satisfied.

Implications of the Dicke Model at MacroQuantum Levels

The Dicke model was developed for quantum optics. However, our (Dotta and Persinger, 2012; Dotta et al, 2013) research suggests that the basic principles and patterns that exist at quantum levels display equivalents within magnetic field exposure systems that employ optocouplers as the primary means by which the circuit is generated (Koren et al, 2015). The physical system described by Dicke is composed of atoms cooperatively interacting with a single mode of an electromagnetic field that is radiating through space-time. This allows for entanglement among multiple particles. For this cooperation to occur one frequency must dominate relative to all others. The resulting rotating wave is an additive (sum) term for the frequency of the cavity in which the atoms occur and the resonant frequency of one of the atoms. According to Garraway's (2011) equations for very large samples of atoms, the uncoupling of the Dicke spin behaves similarly to a giant quantum oscillator. If the atoms are too close dipole-dipole interactions dominant and the symmetry of the Dicke model is compromised.

The containment of the critical components of the effective magnetic fields configurations in the same plane (horizontal) as the cells in culture might be considered a larger scale variant. Although the plate is 6 cm is diameter, with 2.5 cc of cells the thickness would be about 0.9 mm. This might be considered analogous to the "cavity" in the Dicke model. This means that the geometry of the distribution of cells within the magnetic fields is a large sheet where the length of the sheet is about 60 times that of its thickness. The

horizontal magnetic fields would be propagated through this cavity. Several different experiments have indicated that the protons associated with hydronium ion mediate a significant component of the effect. This is based upon the sensitivity of the magnetic field effect to the pH of the solution in which the cells are maintained. Assuming the typical diffusion constant of a proton through the density of cells which display the properties of water to be about ~$0.8 \cdot 10^{-4}$ $cm^2 \cdot s^{-1}$ (DeCoursey, 2003), the frequency associated with a cavity with a depth of 0.9 mm or $0.81 \cdot 10^{-2}$ cm^2 would be ~10^{-2} s or in the order of 1 to 2 min.

This latency is within the range Dotta et al (2014) measured for the emissions of photons from the same type of cell after this particular electromagnetic pattern was applied horizontally across the plates. From this perspective, the influence of the horizontal component containing the effective stimulus configurations from the applied fields upon the constituent cells and the coherence of the small dipoles of the cells through this plane by the Grothuss-like chain movements of protons through the thin sheet (cavity) of cells, may be instrumental in producing the state that promotes photon emissions from the cross-sectional surface. Stated alternatively, the photon emissions would be focused to be emitted perpendicular to the plane through which the charge carriers associated with the magnetic field are moving.

For the Dicke model to be applicable, one mode or frequency must dominate within the large numbers of dipoles (cells) while all others are suppressed. According to our present model the primary involvement of the horizontal plane or thin cavity would be conducive to this condition. The entry of the experimental magnetic fields generated between the two solenoids in the X and the two solenoids in the Y plane could result in generation of waves of protons that begin along the edges of the circular tissue dishes and move towards the center of the plate of cells. Within this focus interference waves and cancellations would occur such that a dominant frequency would occur. Within this umbra the inhibitory effects of the experimental magnetic field on cell growth should be maximal. This is precisely what is observed by microscopic examination. The cell dropout or diminished cell growth is most apparent in the center of the exposed cell plate within a cross-sectional area that is about one-sixth of the area of the total plate.

According to the Dicke model, if the constituent dipoles are too proximal the symmetry is compromised and the coherence exhibits dissolution. The results of our multiple experiments are consistent with this macrospatial manifestation. We have noted that in those instances where the confluence of the cells were greater (i.e., the cell dipoles were statistically closer) at the beginning of the experiment and hence would accelerate the component of the proximal dipole magnitude, the effects of the applied experimental magnetic field were reduced conspicuously. In the Dicke atomic model reducing the volume, enhances coupling strength. At the level of the cell culture very small reductions in the volume containing the same numbers of melanoma cells, results in more consistent values of reduction in malignant cell proliferation (about 30%). The magnitude of the effect is less than the optimal applications (about 50% decrease cell growth).

The specific frequency that would be enhanced in the coherence between the dipoles of cells should exist as a rotating wave which is the sum of the frequency of the cavity mode ω_c and the resonant frequency ω_r of one of the constituents, i.e., a cell and the coupling constant, g, between the proximal cells within the cavity. If we ignore the latter or set the value at unity, the contribution of the voltage potential from which the magnetic field is generated becomes salient. Karbowski et al (2016a) indicated that most powerful diminishments of cell growth

occurred when the application values were 4.3 V. Larger values up to the maximum of 5 V or lower values displayed exponential diminishment to that of no field conditions. Assuming the typical value of $3.6 \cdot 10^{-3}$ cm^2 $V^{-1}s^{-1}$ for diffusion mobility (DeCoursey, 2003), the resulting frequency within the cavity $8.3 \cdot 10^{-3}$ cm^2 would be 1.9 s^{-1} or 0.5 s.

The resonant frequency of the constituents, the cells, might be inferred by the amplitude modulations revealed by the spectral power densities of the photons emitted from these cells. The most consistent spectral peak associated with these emissions is ~22 Hz. If the cavity mode is added the primary mode would be 22 to 23 Hz. This is an important number because it is the upper boundary of the frequency spectra for the experimental field when the point durations composing the field were 3 ms. Point durations that were shorter or longer did not produce the suppression of cell growth and did not enhance calcium transport across the cell membrane (Buckner et al, 2015). Within the Dicke model this interesting observation is rationalized because the 3 ms point duration (only) produced an upper boundary that was congruent with the rotating wave generated within the horizontal plane of cells. Experimental data pair the proton with a 3 ms quantum well-like effect derived from the application of Hubble's parameter (Persinger, 2013).

The importance of frequency mode and the temporal order of that mode should be critical to production of cellular effects. This has been verified by Buckner et al (2015). When the experimental (Thomas) field presentation was reversed (generated backwards) there was no inhibitory effect upon cell growth. If only the beginning (22 Hz) fragment or ending fragment (8 Hz) components were presented to the cells, there was also no effect. From the present perspective such precision must occur. The enhancement of a single mode or frequency through the applied field that would produce the coherent interaction of the cells must occur first before any of the subsequent biochemical reactions and activation of molecular pathways would be initiated. Buckner et al (2015) demonstrated that the likely ion that mediates these effects is calcium through T-type channels. These channels in cell membranes are associated with the electromagnetic properties that govern the latency and thresholds for depolarization or altered resting membrane potentials. In some contexts these channels are associated with "burst firing".

Such relationships had been found independently in the late 20^{th} century by Pilla et al (1999) who investigated the effects of electromagnetic fields on Ca^{2+} CaM-dependent myosin phosphorylation during non-equilibrium stages of the reaction. The rate of the limiting step according to the Michaelis-Menton kinetics showed temporal sensitivities around 1.5 ms or the ½ wavelength equivalent of the optimal 3 ms point duration that is required to produce the malignant cell suppression effects. Two different rates for Ca^{2+} dissociation occurred in a broad range between 10 and 40 Hz which includes the 8 to 24 Hz spectral range of the experimental magnetic field and 300 to 500 Hz or 3.3 ms to 2 ms which again was the optimal point durations for the incremental voltage shifts that produced the magnetic field. They corresponded to the strong and weak Ca^{2+} binding sites on CAM.

Biochemical systems are highly correlative phenomena containing multivariate phenomena. As a result the actual cause may be obscured by shared temporal variances. Some of the more easily detected phenomenon, such as Ca channels, may appear to be the controlling stimulus. However, it may not be the actual (recondite) cause. For example there are more proton channels within most plasma membranes than the sum of all the other types of channels such as potassium or sodium (DeCoursey, 2003). Proton channels are very likely to be coupled to Ca channels in particular (Klockner and Isenberg, 1994; Zhou and Jones,

1996). The conductances of proton channels are strongly pH-dependent. If this is correct than altering the condition of the proton channels which would affect the concentration of H^+ within the cell should affect the efficacy of the applied magnetic field. Our unpublished experiments have shown that an experimentally-induced pH shift extracellular fluid to 6.8 rather than pH 7.4 enhanced the impact of the field upon growth suppression of malignant cells (Murugan et al, 2016).

Photon Emission Coupling to Proton Related pH

Although the concept of quantum optics is a relatively novel application to cell-cell communication the fact that living systems emit photons has been known for decades. Both Popp (2002) and Persinger (2016) have suggested that photon emissions from cells and organisms represent some proportion of the total cumulative energy from flux density from the sun upon the earth's surface over the last 3 billion years. A first order calculation indicates that the total biomass of the earth is the mass-energy equivalence of this solar photon accumulation. Consequently the prominent role of photon emissions in cell-to-cell communication and as controls of biomolecular signalling pathways might be expected. Photon emissions from cell cultures occur during "disequilibrium" or "stress" to the cellular aggregate or system.

Murugan et al's (2016) experiments that showed more inhibition of melanoma growth rates when the extracellular pH was 6.8 compared to 7.4 also indicated the enhanced emission of photons from these cells during the more acidic pH. The increase was equivalent to 250 photons per s from a plate of cells. If the inside of the cell displays a compensatory increase in hydroxyl groups then this emission might be associated with diminishment of proton availability. The digital photomultiplier unit was placed under the plate of cells such that photon emissions would be detected within the aperture. Assuming $4 \cdot 10^{-19}$ J per photon, this would be equivalent to 10^{-16} J per s. There are two solutions from this quantity that couple photons with the movement of protons from the hydronium ions that determine pH. The coupling of the two entities might be considered a condition for the Dicke model to be applied as a macroscopic variant of quantum optics.

First, the typical numbers of melanoma cells within a standard dish is about 0.5 million. The area of the dish is 28 cm^2 while the aperture of the photomultiplier unit is not more than 4 cm^2. Consequently the actual number of cells for which the photons were detected would have been in the order of 10^4 cells. This would mean that for each cell the photonic energy would average about 10^{-20} J per s (Persinger, 2010). This unit of energy is associated with resting membrane potential of cells as was the sequestering of ligands to receptors. One interpretation is this precise range of photon emissions represents the enhanced photon emissions associated with decreased Grotthuss chain movement of protons.

The second calculation involves the number of protons that would be more prominent within the extracellular pH. The difference between pH 7.4 and 6.8 is $\sim 7.2 \cdot 10^{16}$ protons. Assuming the typical volume of a melanoma cells (which is relatively flat in vitro) is 10^{-10} cc, then the displacement outward with the compensatory increase in intracellular pH would be about 10^4 protons per cell. Given the energy for transport of protons through aqueous phases according to DeCoursey (2003) is about 10^{-20} J, the total energy involved per cell would be 10^{-16} J. This is the photon power measured from the approximately 10^4 cells within the photomultiplier unit's aperture. That the same quantity of energy occurs with the movement of protons within a given cell whose numbers and energies match the numbers of total cells

contributing to field is one property of a hologram. In this optic phenomenon the sum of the whole is often equal to the basic unit. This can be considered a form of coherence that is very similar to the properties of a condensate that is usually reserved for very low Kelvin-level temperatures.

Although these quantitative solutions do not prove that the proton movement through the thin layer cavity of sheet of cells is the primary process by which the specific temporal signals within the horizontal components of the applied fields are mediating their cancer-inhibiting effects, the convergent solutions indicate that very small energies and optimal densities of the matter (the protons) contribute to coherence and cooperative interaction. The direct involvement of photons could create the conditions for multi-partite entanglement such that non-local effects could occur across the cells in response to applied magnetic field that would increase the disruption of their growth.

The Role of Copper Metal in Diminishing Beneficial Magnetic Field Effects

The third important result from the direct measurement of the fields is that copper shielding of the solenoids diminished the numbers of excursions within the static magnetic field within the cell exposure area. If these excursions are the essential component that produces the malignant cell suppression, then the recent results reported by Karbowski et al (2016b) are rational. They found that wrapping specific portions of the external area of the solenoids with copper foil completely eliminated the suppression effects of the experimental fields without altering the intensity of the magnetic field within the exposure areas. There are recent calculations that strongly support the ubiquitous role of the Aharanov-Bohm effect in tuned magnetic field-cell electron interactions (Persinger and Koren, 2016).

In addition these researchers found that the relative distance of the exposure chambers (Figure 1) within incubators that contained copper lining or copper shelving was directly related to the efficacy of the experimental (Thomas) field to produce suppression of melanoma growth. Elevating the exposure chambers closer to the copper shelving diminished the effectiveness. Yet in most laboratories these variables are rarely considered. In our experience the physical properties of incubators for cell culture research, which is the dominant method of examination in contemporary biomolecular sciences, are rarely reported. We have measured substantial ranges in the magnetic fields generated within different types of water- or copper-jacketed incubators that can be as intense as the microTesla-level fields employed by experimenters to assess their effects upon cells. This typically non-documented variable could account for the incubator differences and laboratory differences that contribute to the capacity to replicate or not replicate these phenomena.

Murugan et al (2015) had shown that water exposed in the dark to the patterned field employed in the melanoma studies and in the present measurement of parameters resulted in an enhancement of a specific band of photons between 270 and 305 nm.. Aluminum or plastic wrapping of the quantities of spring water during the exposures did not affect this emission. However those quantities of spring water wrapped by copper sheets did not display this emission band. That the effect was specific to ion-containing water, that is spring water that simulates the physiological condition of cells, was demonstrated by the absence of any magnetic field effect upon differential photon emissions when double-distilled water was exposed to the same field conditions. When only spring water was exposed to the malignancy-slowing, patterned magnetic fields serial shifts in pH occurred within increments

of 20 ms to 40 ms (Murugan et al, 2014b) which is remarkably similar to the stacking latency of base nucleotides upon a synthesizing DNA strand.

This band overlaps with the spectroscopic studies of solutes in aqueous solutions reported by Chai et al (2008). They were investigating the long-range interactions between substrates and solvents and discovered the presence of solute free zones near boundaries conditions, exclusion zones, which differentiated this interfacial water from bulk water (Pollack, 2003). The former more typically represents the condition of the cell membrane-water interface. These researchers found an absorption peak within these zones between 250 to 310 nm and fluorescence when excited by 270 nm. Electromagnetic fields can be trapped within atomic aggregates that oscillate in phase with atomic transmissions between ground and excited states reflected by the gap energy (Del Giudice and Preparata, 1994). Karbowski et al (2016c) verified their calculations experimentally. Complex-shaped temporally patterned magnetic fields coherently coupled with (LED) light flashes produced representations of photonic energy within the aqueous suspension of malignant (melanoma) cells. The photons were re-emitted within the subsequent hour after the termination of the field. The total flux power density was directly proportional to the intensity of the magnetic field presented with the light flashes during the first component of the experiment. Interference with the singular modalities that promote theses coherent domains by copper shielding during magnetic field exposures would be expected to eliminate the modality and hence disrupt the coherence.

If the copper shielding eliminated the emission of the marker for the exclusion zone (EZ) pursued by Pollack over the last three decades (2003), then two implications arise. First, the parallel single modality within the optic range for the Dicke model would involve the 270 nm wavelength. If it is blocked by the quantum consequences of copper shielding then the cooperative dipole coherence between the cells would not occur. Interfacial water has a number of characteristics that could promote cooperation between adjacent cells within the cavity. First adjacent to the surface (such as the membrane) there is a 10 fold increase in viscosity. Very specific physical chemistry within water would set the condition for enter of zero point potential oscillations into the local reaction (Persinger, 2015). Second, and most critically, the separation between the EZ and bulk water near a surface contain a sheet of concentrated protons. The potential difference associated with this sheet ranges in the order of 100 mV which is the same order of magnitude as the plasma cell membrane. Thus the presence of the high density of protons within interface between interfacial and bulk water might be considered a cavity through which further coherence would occur across the cells in the same plane as the horizontal magnetic field.

To date there are only two major means by which to treat and to diminish cancer growth. They are intense ionizing radiation and chemical therapies. Both destroy or disrupt normal cells as well as cancer cells. Both are intrusive, disruptive techniques that operate primarily upon those cells with the greater division rates or metabolic activity. The potential of the third option, temporally-patterned magnetic fields applied to the entire organism, is that only malignant cells are affected while normal cells are not. The third treatment is not dependent upon blood flow or technology to focus irradiative beams within the volume of the body. However what the third treatment does require is the precise information to switch on and switch off molecular pathways that is comparable to the precision and discrete energies that define quantum phenomena.

ACKNOWLEDGEMENTS

Thanks to Dr. W. E. Bosarge and the Bosarge Family Organization for the support of the research that has led to these discoveries.

References

[1] Adair, R. K. (1991). Constraints on biological effects of weak extremely-low-frequency electromagnetic fields. Physical Review A, 43(2), 1039.

[2] Adey, W. R. (1981). Tissue interactions with nonionizing electromagnetic fields. Physiological Reviews, 61(2), 435-514.

[3] Afsharimani, B., Cabot, P., and Parat, M. O. (2011). Morphine and tumor growth and metastasis. Cancer and Metastasis Reviews, 30(2), 225-238.

[4] Berg, H. (1999). Problems of weak electromagnetic field effects in cell biology. Bioelectrochemistry and Bioenergetics, 48(2), 355-360.

[5] Buckner, C. (2012). Effects of electromagnetic fields on biological processes are spatial and temporal-dependent. Library and Archives Canada.

[6] Buckner, C. A., Buckner, A. L., Koren, S. A., Persinger, M. A. and Lafrenie, R. M. (2015). Inhibition of cancer cell growth by exposure to specific time-varying electromagnetic field involves T-type channels. PLOS ONE, DOI: 10.1371.

[7] Burke, H. E. (1986). Handbook of magnetic phenomena. Van Nostrand Reinhold: N.Y.

[8] Chai, B-h, Zheng, J.-m., Zhao, Q., and Pollack, G. H. (2008). Spectroscopic studies of solutes in aqueous solution. Journal of Physical Chemistry, 112, 2242-2247.

[9] DeCoursey T.E. (2003). Voltage-gated proton channels and other proton transfer pathways. Physiol. Rev. 83, 476-579

[10] Del Giudice, E. and Preparata, G. (1994). Coherent dynamics in water as a possible explanation of biological membranes formation. Journal of Biological Physics, 20, 105-116.

[11] Dotta, B. T. and Persinger, M. A. (2012). "Doubling" of local photon emissions when two simultaneous, spatially separated, chemiluminescent reactions share the same magnetic field configurations. Journal of Biophysical Chemistry, 3, 72-80.

[12] Dotta, B. T., Murugan, N. J., Karbowski, L. M. and Persinger, M. A. (2013). Excessive correlated shifts in pH with distal solutions sharing phase-uncoupled angular accelerating magnetic fields: macro-entanglement and information transfer. International Journal of Physical Sciences, 8, 1783-1787.

[13] Dotta, B. T., Lafrenie, R. M., Karbowski, L. M., and Persinger, M. A. (2014). Photon emission from melanoma cells during brief stimulation by patterned magnetic fields: is the source coupled to rotational diffusion within the membrane. General Physiology and Biophysics, 33, 63-73.

[14] Garraway, B. M. (2011). The Dicke model in quantum optics: Dicke model revisited. Philosophical Transactions of the Royal Society A, 369, 1137-1155.

[15] Hu, J. H., St-Pierre, L. S., Buckner, C. A., Lafrenie, R. M., and Persinger, M. A. (2010). Growth of injected melanoma cells is suppressed by whole body exposure to specific spatial-temporal configurations of weak intensity magnetic fields. International journal of radiation biology, 86(2), 79-88.

[16] Karbowski, L. M., Harribance, S. L., Buckner, C. A., Mulligan, B. P., Koren, S. A., Lafrenie, R. M. and Persinger, M. A. (2012). Digitized quantitative electroencephalographic patterns applied as magnetic fields inhibit melanoma cell proliferation in culture. Neuroscience Letters, 523(2), 131-134.

[17] Karbowski, L.M., Murugan, N.J., Koren, S. A. and Persinger, M.A. (2015a). Seeking the source of transience for a unique magnetic field pattern that completely dissolves cancer cells in vitro. Journal of Biomedical Science and Engineering, 8, 531-543.

[18] Karbowski, L.M., Murugan, N.J., Lafrenie, R.M., and Persinger, M.A. (2016a). Experimental demonstration that Aharanov-Bohm phase shift voltages in optical coupler circuits of tuned patterned magnetic fields is critical for inhibition of malignant cell growth. Journal of Advances in Physics, 11(7), 3557-3563.

[19] Karbowski, L. M., Murugan, N. J., Lafrenie, R. M. and Persinger, M. A. (2016b). Elimination of growth inhibition of malignant cells by specific patterned magnetic fields when source solenoids are wrapped with copper: implications for quantum (Aharanov-Bohm) effects (in submission).

[20] Karbowski, L. M., Murugan, N. J. and Persinger, M. A. (2016c). Experimental evidence that specific photon energies are "stored" in malignant cells for an hour: the synergism of weak magnetic field-LED wavelength pulses. Biology and Medicine, 8:1.

[21] Klockner, U. and Isenberg, G. (1994). Calcium channel current of vascular smooth muscle cells: extracellular protons modulate gating and single channel conductance. Journal of General Physiology, 103, 665-678.

[22] Koren, S. A., Bosarge, W. E. and Persinger, M. A. (2015). Magnetic fields generated by optical coupler circuits may also be containment loci for entanglement of PN junction-plasma cell membrane photons within exposed living systems. International Letters of Chemistry, Physics and Astronomy, 3, 84.

[23] Litovitz, T. A., Penafiel, M., Krause, D., Zhang, D. and Mullins, J. M. (1997). The role of temporal sensing in bioelectromagnetic effects. Bioelectromagnetics, 18, 388-395.

[24] Martin, L. J., Koren, S. A. and Persinger, M. A. (2004). Thermal analgesic effects from weak, complex magnetic fields and pharmacological interactions. Pharmacology, Biochemistry and Behavior, 78, 217-227.

[25] Murugan, N. J., Karbowski, L. M. and Persinger, M. A. (2014a) Weak burst-firing magnetic fields that produce analgesia equivalent to morphine do not initiate activation of proliferaition pathways in human breast cells in culture. Integrative Cancer Science and Therapeutics, 1, 47-50.

[26] Murugan, N. J., Karbowski, L. M. and Persinger, M. A. (2014b). Serial pH increments (20 to 40 milliseconds) in water during exposures to weak, physiologially-patterned magnetic fields: implications for consciousness. Water, 6, 45-60.

[27] Murugan, N. J., Karbowski, L. M., Lafrenie, R. M. and Persinger, M. A. (2015). Maintained exposure to spring water but not double distilled water in darkness and thixotropic conditions to weak (1 microTesla) temporally patterned magnetic fields shift photon spectroscopic wavelengths: effects of different shielding materials. Journal of Biophysical Chemistry, 6, 14-28.

[28] Murugan, N. J., Karbowski, L. M., Lafrenie, R. M. and Persinger, M. A. (2016). Small shifts in extracellular pH in melanoma cells elicit marked increases photon emission: a potential role for proton channels. (in submission).

[29] Murugan, N. J., Karbowski, L. M., & Persinger, M. A. (2014). Serial pH Increments (~ 20 to 40 Milliseconds) in Water during Exposures to Weak, Physiologically Patterned Magnetic Fields: Implications for Consciousness.Water, 6, 45-60.

[30] Persinger, M. A. (2010). 10^{-20} Joules as neuromolecular quantum in medicinal chemistry: an alternative approach to myriad molecular pathways. Current Medicinal Chemistry, 8, 1957-1969.

[31] Persinger, M. A. (2013). Experimental evidence that Hubble's Parameter could be reflected in local physical and chemical reactions: support for Mach's principle of imminence of the universe. International Letters of Chemistry, Physics and Astronomy, 11, 86-92.

[32] Persinger, M. A. (2015). Thixotropic phenomena in water: quantitative indicators of Casimir-magnetic transformations from vacuum oscillations (virtual particles). Entropy, 17, 6200-6212.

[33] Persinger, M A. (2016). Spontaneous photon emissions in photoreceptors: potential convergence of Arrhenius reactions and the latency for rest mass photons to accelerate to Planck unit energies. Journal of Advances in Physics, 11, 3529-3537.

[34] Persinger, M. A. and Koren, S. A. (2016). The Aharanov-Bohm phase shift and magnetic vector potential A could accommodate for optical coupler, digital-to-analogue magnetic field excess correlations of photon emissions within living aqueous systems. Journal of Advances in Physics, 11, 3333-3339.

[35] Pilla, A. A., Muesham, D. J., Markov, M. S. and Sisken, B. F. (1999) EMF signals and ion/ligand binding kinetics: prediction of bioeffective waveform parameters. Bioelectrochemistry and Bioenergetics, 48, 27-34.

[36] Pollack, G. H. (2003). The role of aqueous interfaces in the cell. Advanves of aqueous interfaces in the cell. Advances in Colloid and Interface Science, 103, 173-196.

[37] Popp, F. A., Chang, J. J., Herzog, A., Yan, Z. and Yan, Y. (2002). Evidence of non-classical (squeezed) light in biological systems. Physics letters A, 293(1), 98-102.

[38] Rouleau, N. and Persinger, M. A. (2015). Local electromagnetic fields exhibit temporally non-linear, east-west oriented 1-5 nT diminishments with a toroid: empirical

measurements and quantitative solutions indicating a potential mechanism for excess correlation. Journal of Electromagnetic Analysis and Applications, 7, 19-30.

[39] Rouleau, N., Carniello, T. N. and Persinger, M. A. (2016). Identifying Factors Which Contribute to the Magnitude of Excess Correlations between Magnetic Field-Paired Volumes of Water. Journal of Signal and Information Processing, 7(03), 136.

[40] Tonomura, A., Osakabe, N., Matsuda, T., Kawasaki, T., Endo, J., Yano, S. and Yamada, H. (1986). Evidence for Aharonov-Bohm effect with magnetic field completely shielded from electron wave. Physical Review Letters, 56(8), 792.

[41] Vares, D.A.E., Corradini, P.L. and Persinger, M.A. (2016). MicroVolt variations of the human brain (quantitative electroencephalography) display differential torque effects during West-East vernus North-South Orientation in the geomagnetic field. Journal of Advances in Physics, 12(2), 4255-4259.

[42] Zhadin, M. N., Novikov, V. V., Barnes, F. S. and Pergola, N. F. (1998). Combined action of static and alternating magnetic fields on ionic current in aqueous glutamic acid solution. Bioelectromagnetics, 19, 41-45.

[43] Zhou, W. and Jones, S. W. (1996). The effects of external pH on calcium channel currents in bullfrog sympathetic neurons. Biophysical Journal, 70, 1326-1334.

(Received 16 August 2016; accepted 04 September 2016)